Cell

In Vivo Two-Photon Imaging Reveals a Role of Arc in Enhancing Orientation Specificity in Visual Cortex

Kuan Hong Wang,[1,2,3,4,5] Ania Majewska,[2,5] James Schummers,[2,5] Brandon Farley,[2,5] Chengcheng Hu,[6] Mriganka Sur,[2,5] and Susumu Tonegawa[1,2,3,4,5,*]
[1] Howard Hughes Medical Institute
[2] The Picower Institute for Learning and Memory
[3] RIKEN-MIT Neuroscience Research Center
[4] Department of Biology and
[5] Department of Brain and Cognitive Sciences
Massachusetts Institute of Technology, Cambridge, MA 02139, USA
[6] Department of Biostatistics, Harvard School of Public Health, Boston, MA 02115, USA
*Contact: tonegawa@mit.edu
DOI 10.1016/j.cell.2006.06.038

SUMMARY

Cortical representations of visual information are modified by an animal's visual experience. To investigate the mechanisms in mice, we replaced the coding part of the neural activity-regulated immediate early gene Arc with a GFP gene and repeatedly monitored visual experience-induced GFP expression in adult primary visual cortex by in vivo two-photon microscopy. In Arc-positive GFP heterozygous mice, the pattern of GFP-positive cells exhibited orientation specificity. Daily presentations of the same stimulus led to the reactivation of a progressively smaller population with greater reactivation reliability. This adaptation process was not affected by the lack of Arc in GFP homozygous mice. However, the number of GFP-positive cells with low orientation specificity was greater, and the average spike tuning curve was broader in the adult homozygous compared to heterozygous or wild-type mice. These results suggest a physiological function of Arc in enhancing the overall orientation specificity of visual cortical neurons during the post-eye-opening life of an animal.

INTRODUCTION

Neurons in the primary visual cortex respond most intensively to edges of light at specific orientations (Hubel and Wiesel, 1962). The initial establishment of this orientation selectivity does not require visual input; some orientation selective neurons are already present at the time of eye opening after birth (Hubel and Wiesel, 1963). However, the overall orientation selectivity of the neurons in the primary visual cortex is enhanced by visual experience in the juvenile animals (Chapman et al., 1999; Crair et al., 1998; White et al., 2001). In adults, daily practice of orientation identification tasks can further improve orientation selectivity (Schoups et al., 2001).

To investigate the cellular mechanisms of experience-dependent changes in orientation selectivity, it would be desirable to repeatedly monitor the responses of the same population of neurons at single-cell resolution over a prolonged period of time (days). However, orientation selectivity has traditionally been determined by recording single-unit spiking activities with extracellular microelectrodes (Hubel and Wiesel, 1963), which does not allow repeated sampling of the same cells. Optical imaging of intrinsic metabolic signals has been used to follow orientation preference maps in the same animals (Chapman et al., 1999), but this technique does not have single-cell resolution.

At the molecular level, relatively little is known about the factors contributing to experience-dependent changes in orientation selectivity. Genetic elimination of NMDA receptor subunit 2A (NR2A) or postsynaptic scaffold protein PSD-95 reduced orientation selectivity, as indicated by single-unit recordings (Fagiolini et al., 2003), raising the possibility that signaling through NMDA receptors may be essential for the induction of orientation plasticity. However, it is not known what molecules may mediate the expression of these plastic changes.

In order to circumvent some of the shortcomings of those approaches adopted previously, we combined in vivo two-photon microscopy with mouse genetic engineering. Two-photon microscopy offers the opportunity to chronically track fluorescent markers in the same neurons for many days in live animals (Grutzendler et al., 2002; Trachtenberg et al., 2002). To construct a genetically

encoded optical reporter of a cellular response to neuronal stimulation, we created a strain of mouse in which a GFP gene replaced the coding part of the immediate early gene Arc. In this strain of mouse, GFP expression is under the control of the endogenous Arc promoter, which is activated by neuronal stimulation in forebrain regions (Link et al., 1995; Lyford et al., 1995). In visual cortex, Arc gene is inactive until after eye opening, and thereafter becomes rapidly activated by visual stimulation (Lyford et al., 1995; Tagawa et al., 2005). Interruption of synaptic input to primary visual cortex has been shown to prevent this post-eye-opening activation of the Arc gene (Lyford et al., 1995; Tagawa et al., 2005). In addition, pharmacological blockade of NMDA receptors completely abolishes Arc expression (Link et al., 1995; Lyford et al., 1995; Steward and Worley, 2001b). Thus, the expression of Arc promoter-driven GFP (Arc-GFP) could be used as a reporter of neural activity-regulated, NMDA receptor-dependent cellular response. Although the relationship between Arc expression and firing of action potentials has not been entirely elucidated (Guzowski et al., 1999; Guzowski et al., 2006), we monitored Arc-GFP expression in individual neurons and refer to this as neuronal activation throughout the paper.

The in vivo physiological functions of Arc protein have thus far remained largely unknown. Electron microscopic analysis revealed that Arc protein can preferentially localize to excitatory synapses in recently activated dendritic segments, while biochemical studies showed the association of Arc with protein complexes present in the postsynaptic density (Moga et al., 2004; Steward and Worley, 2001a). Additionally, injection of Arc antisense oligonucleotides into the hippocampus appears to reduce the maintenance of LTP (Guzowski et al., 2000). Together, these observations suggest that Arc may be important for neuronal plasticity. However, whether or not Arc protein plays a role in orchestrating cortical ensembles activated by natural sensory stimuli has not been investigated.

Here, we show that Arc-GFP expression was induced in distinctive neuronal ensembles by horizontally or vertically oriented visual stimuli in the primary visual cortex of Arc-GFP heterozygous mice. These ensembles became progressively smaller and more reliable for reactivation as the same animal was repeatedly exposed to the stimuli over the period of a week. This adaptation process was not affected by the lack of Arc in Arc-GFP homozygous mice. However, the GFP+ population in the homozygous mice was larger than that in the heterozygous mice and this difference was due to an occurrence of a greater number of cells with relatively low orientation specificity in the homozygous mice. These imaging data were corroborated by the single-unit microelectrode recording data showing that on average, Arc-lacking cells in the homozygous mice had reduced orientation selectivity and broadened orientation tuning response. Taken together, our study has revealed the existence of two separable experience-dependent visual cortical plasticity processes; one is Arc-dependent enhancement of orientation specificity operating during the post-eye opening life, and the other is Arc-independent adaptation process operating in an adult animal while it is repeatedly exposed to a given visual stimulus.

RESULTS

Generation and Characterization of Arc-GFP Knockin Mice

To begin to investigate the mechanisms underlying experience-dependent cortical information processing, we developed an Arc-GFP knockin mouse line. In order to generate a faithful reporter of Arc promoter activity, the DNA construct containing the GFP coding sequence was inserted after the ATG start codon of the endogenous Arc gene through homologous recombination in embryonic stem cells (Figure 1A). The targeting of GFP into the Arc genomic locus was confirmed by southern blot (data not shown) and PCR analysis (Figure 1B). Mice were normally reared until 2–3 months of age before the start of experiments. The level of Arc protein in brain extracts was undetectable in the homozygous mice (Figure 1B), while it was reduced by only 20% in the heterozygous mice compared to the wild-type mice (het/wt: 0.80 ± 0.10 SE, $n = 4$, see Experimental Procedures). Functionally, this small reduction of Arc protein level in the heterozygous mice did not seem to affect their visual responses (Figures 7B–7D). To confirm that the expression of GFP coincides with that of the endogenous Arc protein in the heterozygous mice, we exposed these mice to a lighted environment, then two hours later, performed double immunofluorescent staining with antibodies specific for Arc and GFP on sections of primary visual cortex. We observed that the majority of the Arc and the GFP signals indeed overlapped (Figure 1C). Under the same experimental condition, GFP was expressed in the homozygous mice, but Arc protein was not detectable (Figure 1C).

In order to report the dynamic regulation of Arc promoter by neural activity, a destabilized form of GFP (d2EGFP) was used in the targeting construct. The half-life of d2EGFP is shortened to approximately two hours (Li et al., 1998), comparable to the decay time of Arc protein (Wallace et al., 1998). In addition, the degradation of d2EGFP is not affected by neural activity (Sutton et al., 2004). To characterize the time course of Arc-GFP induction in primary visual cortex, we examined the GFP signals on brain sections at various time points after briefly exposing dark-adapted mice to a visual environment. We found that the GFP signals from previous visual experience were absent after overnight (20 hr) dark adaptation (Figure 2A), same as the Arc gene expression (Tagawa et al., 2005). The newly induced GFP signals reached a peak level approximately 2 hr after visual stimulation, and disappeared 12 hr later (Figure 2A). To examine the dependency of GFP induction in primary visual cortex on visual inputs, we exposed the Arc-GFP mice to a novel chamber in complete darkness. GFP signals were not induced in primary visual cortex under this condition (Figure 2B). Therefore, visual

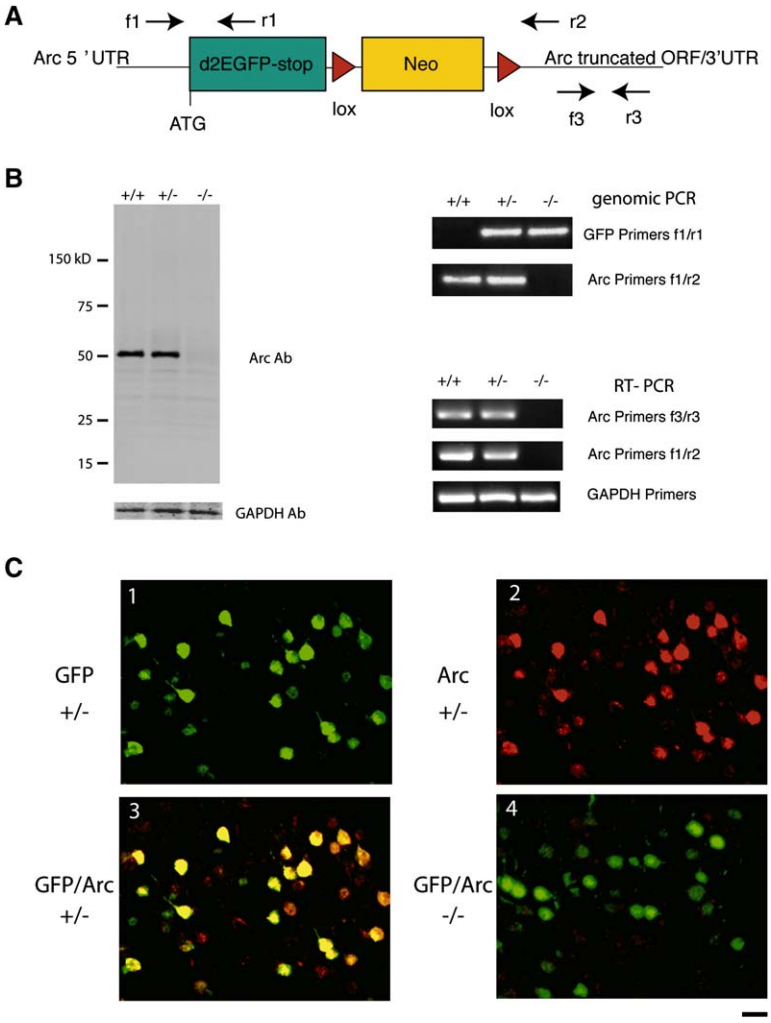

Figure 1. Generation and Characterization of Arc-GFP Knockin Mice

(A) Diagram of the gene-targeting construct.

(B) Arc protein production was completely disrupted in the homozygous mice, as shown by Western blot analysis of brain extracts (left panel). The expression level of a house-keeping enzyme GAPDH was used as a sample loading control. The genotypes of mice were shown by PCR analysis (upper right panel). The disruption of Arc mRNA expression in homozygous mice was shown by RT-PCR analysis of brain total RNA preparation (lower right panel). The positions of primers are shown in (A).

(C) Double immunofluorescent staining of Arc (red) and GFP (green) in the visual cortex of Arc-GFP mice that were visually stimulated. GFP and Arc were expressed in the same cells in the heterozygous mice (1, 2, 3), whereas Arc was not expressed in the homozygous mice (4), as shown in separate (1, 2) and overlaid (3, 4) channels. The scale bar represents 20 μm.

inputs are required for the Arc-GFP response. To examine the dependency of Arc-GFP response on NMDA receptor mediated neural activity, we administered the NMDA receptor antagonist MK-801 to Arc-GFP mice. After drug administration, visual stimulation failed to induce GFP signals (Figure 2B). Taken together, the induction of Arc-GFP by visual inputs reflects an NMDA receptor-dependent response of the endogenous Arc promoter in primary visual cortex.

In Vivo Imaging of Arc-GFP Induction by Visual Stimulation

We next adapted an in vivo two-photon imaging method (Majewska and Sur, 2003) to repeatedly monitor the expression of Arc-GFP in the brain of live mice. Normally reared Arc-GFP mice at 2–3 months of age were implanted with transparent cranial windows over the primary visual cortex. Before the start of the first imaging session, an Arc-GFP mouse was housed in dark overnight for 20 hr (Figure 3A). It was then exposed to a salient visual stimulus in an unrestrained environment for 15 min. Two hours later, when the induction of Arc-GFP would have reached its peak level, the mouse was anesthetized and placed on a microscope stage for two-photon imaging of the superficial layers of primary visual cortex. Both the unique vasculature patterns and stable auto-fluorescent signals were used as alignments for repeated imaging of the same animal (Figure 3B and Experimental Procedures).

Reliability and Experience-Dependence of Arc-GFP Response during Repeated Visual Exposures

To examine whether Arc-GFP signals reliably report the same visual experience in repeated exposures, we imaged the expression of Arc-GFP in heterozygous mice in response to a constant visual environment once per day for six consecutive days. To control the properties of the visual stimulus, we designed a visual environment consisting of a cylinder covered with alternating black and white stripes of equal widths aligned in either a horizontal or a vertical orientation. Video monitoring confirmed that the mice freely explored the environment during the 15 min exposure time, and showed no neck torsions that

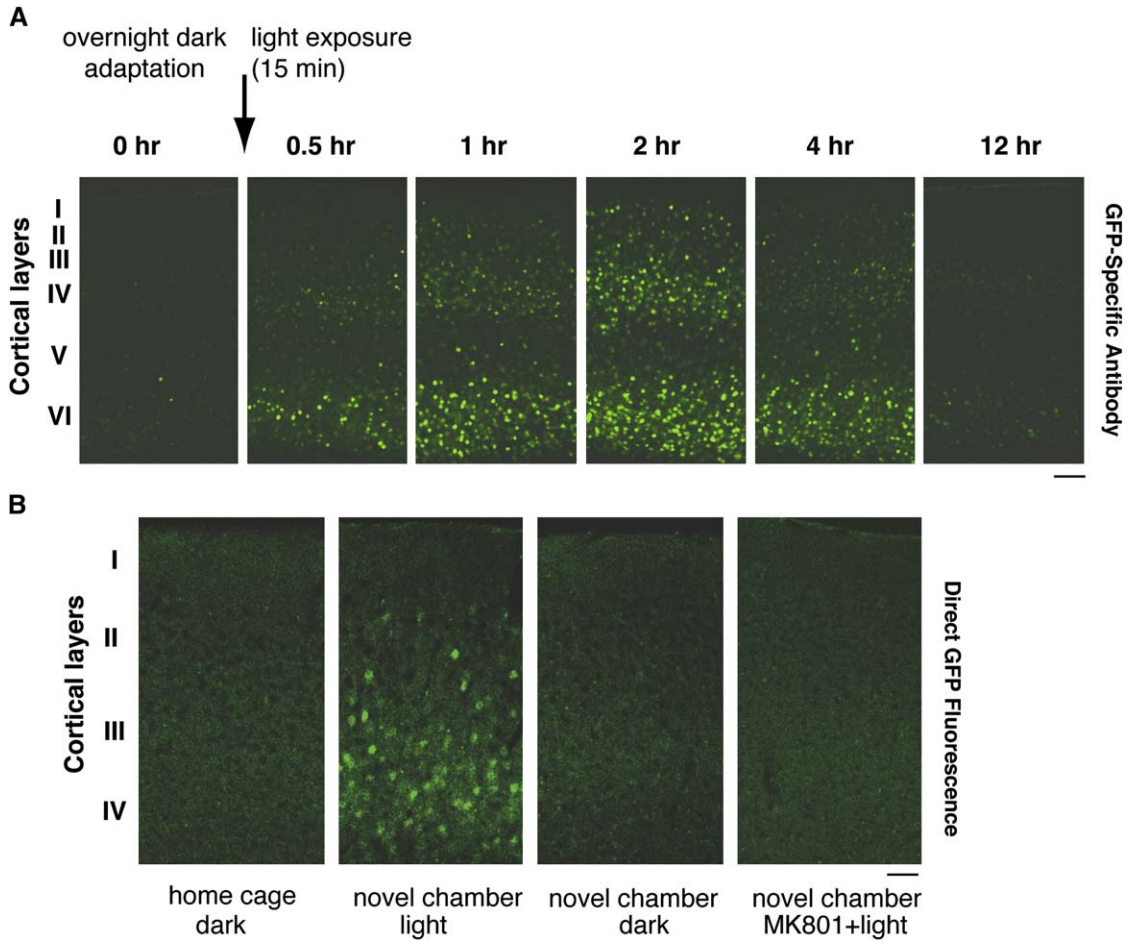

Figure 2. The Dynamics and Specificity of Arc-GFP Activation by Visual Input

(A) Heterozygous Arc-GFP knockin mice were dark adapted for 20 hr, then exposed to a visual environment for 15 min. Afterwards, the mice were returned to their home cages in the dark, and sacrificed at 0.5, 1, 2, 4, and 12 hr later. Time point 0 refers to mice sacrificed before light stimulation. GFP expression in those mice was detected by immunofluorescent staining on fixed sections of primary visual cortex, using GFP-specific antibody. The scale bar represents 100 μm.

(B) Detection of GFP-expressing cells by confocal microscopy on fixed sections of the superficial layers of primary visual cortex. GFP-expressing cells were not observed in any superficial layers after mice were dark adapted overnight in their home cages (1). GFP-expressing cells were detected in layers II, III, and IV 2 hr after mice were exposed to light in a novel chamber (2). Exposure to a novel chamber in the dark (3) or exposure to a novel chamber in light 30 min after intraperitoneal injection of 1 mg/kg NMDA receptor antagonist MK-801 (4) did not lead to GFP induction. The scale bar represents 40 μm.

would distort the stimulus orientation (data not shown). Such visual environments have been used effectively before to restrict visual experience to a single orientation in kittens (Sengpiel et al., 1999).

When images of the same cortical region from two consecutive days were examined, the patterns of activated neurons appeared to be quite similar (Figure 3B). But fewer neurons were activated on day 2 than that on day 1 (Figure 3B). Quantitative image analysis showed that there was a clear reduction in the number of GFP+ neurons after repeated exposure to the stripes of the same orientation, regardless whether the stripes were horizontally or vertically oriented (Figure 3C). However, the number of GFP+ neurons increased to the day 1 level in response to a new stimulus (Figure 3D), suggesting that the reduction in cell number is specific to the repeated visual stimulus. These data also show that the reduction in cell number is not due to the dark rearing between the daily light exposure sessions, or the anesthesia treatments during the microscopic observation. To further understand how the reduction of GFP+ neurons is driven by repeated experience, we constructed a tree graph to trace the reactivation probabilities of neurons based on their prior activation history (Figure 3E, "activation" refers to Arc-GFP expression). Strikingly, we observed that the neurons that were consistently activated before became more likely to be reactivated (Figure 3F), while those that were consistently inactive before became more likely to

remain silent (Figure 3G). Therefore, repeated exposures to the same stimulus led to the reactivation of a progressively smaller population of cells with greater reactivation reliability.

Orientation Specificity of Arc-GFP Response

We next investigated whether Arc-GFP activation patterns consistently report stimulus orientation. Arc-GFP heterozygous mice were exposed to horizontal or vertical stripes on alternate days for a total of six days. Distinctive activation patterns of Arc-GFP were observed in response to different orientations (Figure 4A). The percentage of day 1 GFP+ neurons that were reactivated on subsequent days was consistently higher on days 3 and 5 when the stimulus orientation was the same as day 1, than that on days 2, 4, and 6 when the stimulus orientation was orthogonal to day 1 (Figure 4B). Similarly, the percentage of day 2 GFP+ neurons that were reactivated on subsequent days also correlated with the stimulus orientation (Figure 4C). Taken together, we conclude that the Arc-GFP signals reveal orientation specific neuronal responses in primary visual cortex.

More GFP+ Neurons Activated by a Single Orientation in Arc Knockout Mice

Our data on the orientation specific Arc-GFP responses provide direct cellular snapshots of experience-dependent information processing in visual cortex (Figures 3C–3G, 4B, and 4C). The Arc-GFP knockin mouse line therefore offers a genetic system to examine the mechanisms underlying the experience-dependent and orientation-specific activation of neuronal ensembles in primary visual cortex. In particular, in the homozygous Arc-GFP mice, Arc protein is not produced, but GFP is still expressed under the control of Arc promoter (Figures 1B and 1C). To investigate Arc protein function, we compared the GFP expression patterns in the Arc-GFP homozygous mice to those in the heterozygous mice at 2–3 months of age with normal rearing conditions before the start of imaging experiments. We first tallied the number of GFP+ neurons in each imaged brain region that were activated by a single orientation presented on experimental day one (Figure 5A). Interestingly, there were more GFP+ neurons in the homozygous than that in the heterozygous mice (Figure 5A, $p < 0.001$, $n = 24$). To determine whether this difference might be due to an increase of fluorescence intensity (calculated as the ratio between the soma GFP signal and its surrounding background, see Experimental Procedures) in the homozygous mice, which have two copies of the GFP gene rather than one copy as in the heterozygous mice, we compared the intensity distribution of GFP+ neurons in those mice. There were more GFP+ neurons in the homozygous mice than in the heterozygous mice across the whole range of intensity levels (Figure 5B). On the other hand, the mean intensity level did not change significantly between the two genotypes (Het: 2.77 ± 0.06 SE, Hom: 2.92 ± 0.10 SE, $p = 0.21$, t test, $n = 24$). Thus, the larger population of GFP+ neurons activated by a single orientation in the Arc homozygous mice did not seem to be caused by a shift in fluorescence intensity.

Normal Reactivation Probability of GFP+ Neurons during Repeated Exposures to the Same Orientation in Arc Knockout Mice

We next examined a potential role of Arc in regulating the reactivation probabilities of GFP+ neurons during the SAME orientation exposure paradigm (as in Figures 3F and 3G). Although there were more activated neurons in the homozygous than the heterozygous mice on each of the exposure days (Figure 5C), the numbers of activated neurons decreased with repeated exposures in the homozygous mice as in the heterozygous mice. When we compared the dependence of Arc-GFP reactivation probability on prior activation histories (Figures 5D and 5E), we found no significant difference between the two genotypes ($p > 0.05$, $n = 12$ regions, repeated measures two-way ANOVA). Therefore, Arc protein does not seem to be important for regulating the reactivation probabilities of GFP+ neurons during repeated exposures to the same orientation.

Reduced Orientation Specificity of the Patterns of GFP+ Neurons in Arc Knockout Mice

We then studied the effect of Arc knockout on the orientation specificity of the patterns of GFP+ neurons in the alternate-orientation exposure paradigm (as in Figures 4B and 4C). The shapes of reactivation curves were significantly different between the heterozygous and homozygous mice (Figures 5F and 5G, $p < 0.0001$, $n = 12$ regions, repeated measures two-way ANOVA). In particular, the percentage of day 1 GFP+ neurons reactivated by exposure to the orthogonal orientation (on day 2, 4, and 6) was significantly higher in the homozygous compared to the heterozygous mice (Figure 5F, $p < 0.001$, with correction for multiple comparison). By contrast, the percentage of neurons reactivated by exposure to the same orientation (on day 3 and 5) was not significantly different between the two genotypes (Figure 5F, $p > 0.05$). Therefore, the orientation specificity of the patterns of GFP+ neurons was reduced in Arc knockout mice.

Increased Numbers of GFP+ Neurons with Relatively Low Orientation Specificity in Arc Knockout Mice

To investigate how the loss of Arc function affects the responses of individual neurons in more details, we classified GFP+ neurons into nine groups based on the pattern of their responses to horizontal and vertical stripes during the 6-day alternate-orientation experiment. Surprisingly, the numbers of cells that responded once, twice or three times to one specific orientation, but never to the other orientation (labeled as 1:0, 2:0, 3:0, respectively), were not significantly different between the heterozygous and homozygous mice (Figure 6A, $p > 0.05$, t test, $n = 12$). By contrast, the numbers of cells that responded to both orientations (3:3, 2:2, 1:1, 3:2, 2:1 and 3:1) were significantly higher in the homozygous than the heterozygous mice

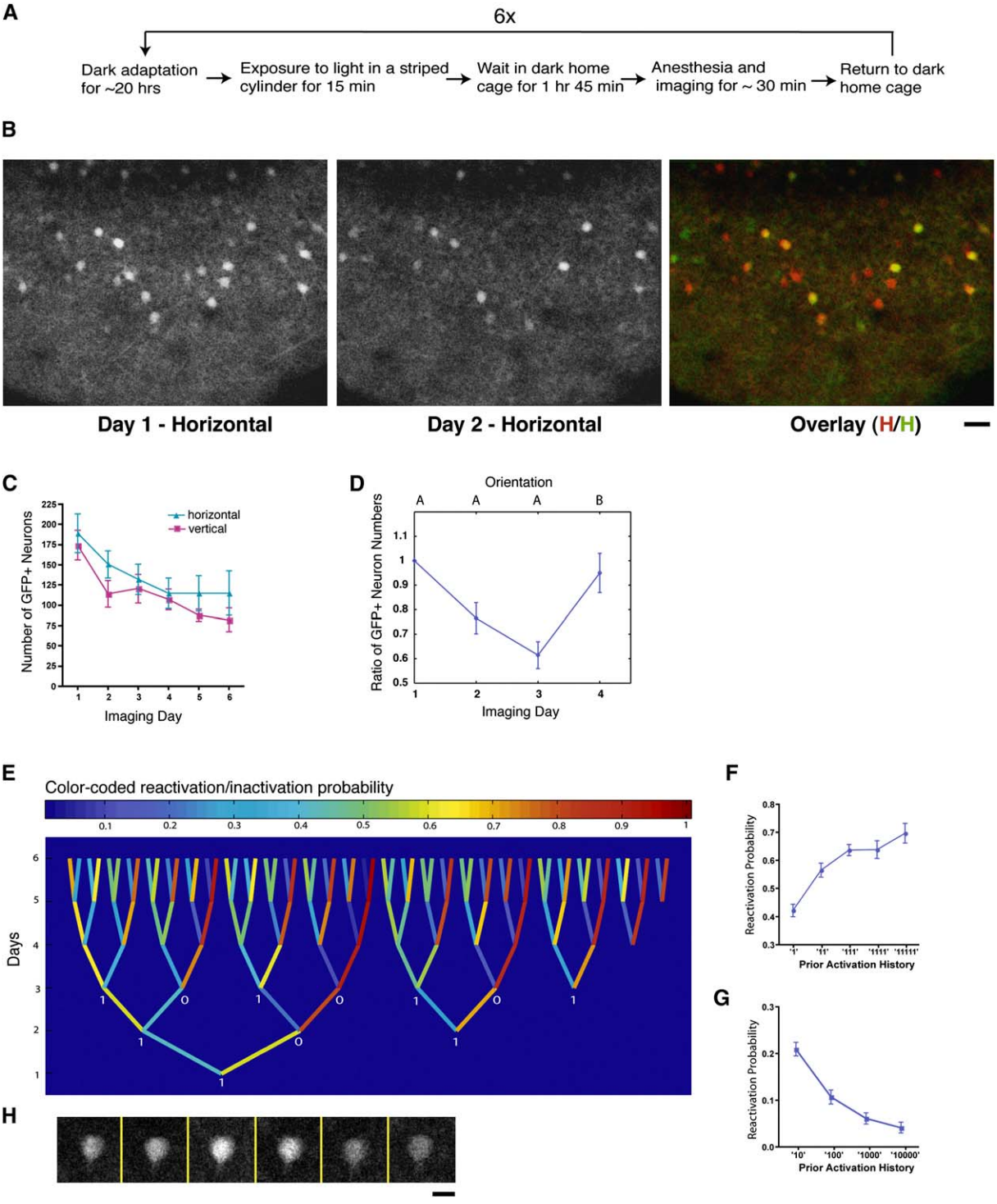

Figure 3. Reliability and Experience Dependence of Arc-GFP Response

(A) A flow chart of behavioral stimulation and imaging procedures.

(B) The alignment of two-photon images taken from the superficial primary visual cortical layers in heterozygous Arc-GFP mice stimulated by the same orientation on two consecutive days shows the reduction in the number of GFP+ neurons. The scale bar represents 30 μm.

(C) A gradual reduction in the number of GFP+ neurons in response to either horizontal or vertical stimulations. There is no significant difference between the two orientations ($p > 0.05$), but experience has a significant effect ($p < 0.0001$, repeated measures two-way ANOVA, n = 6 regions, two regions per animal, three mice in each orientation).

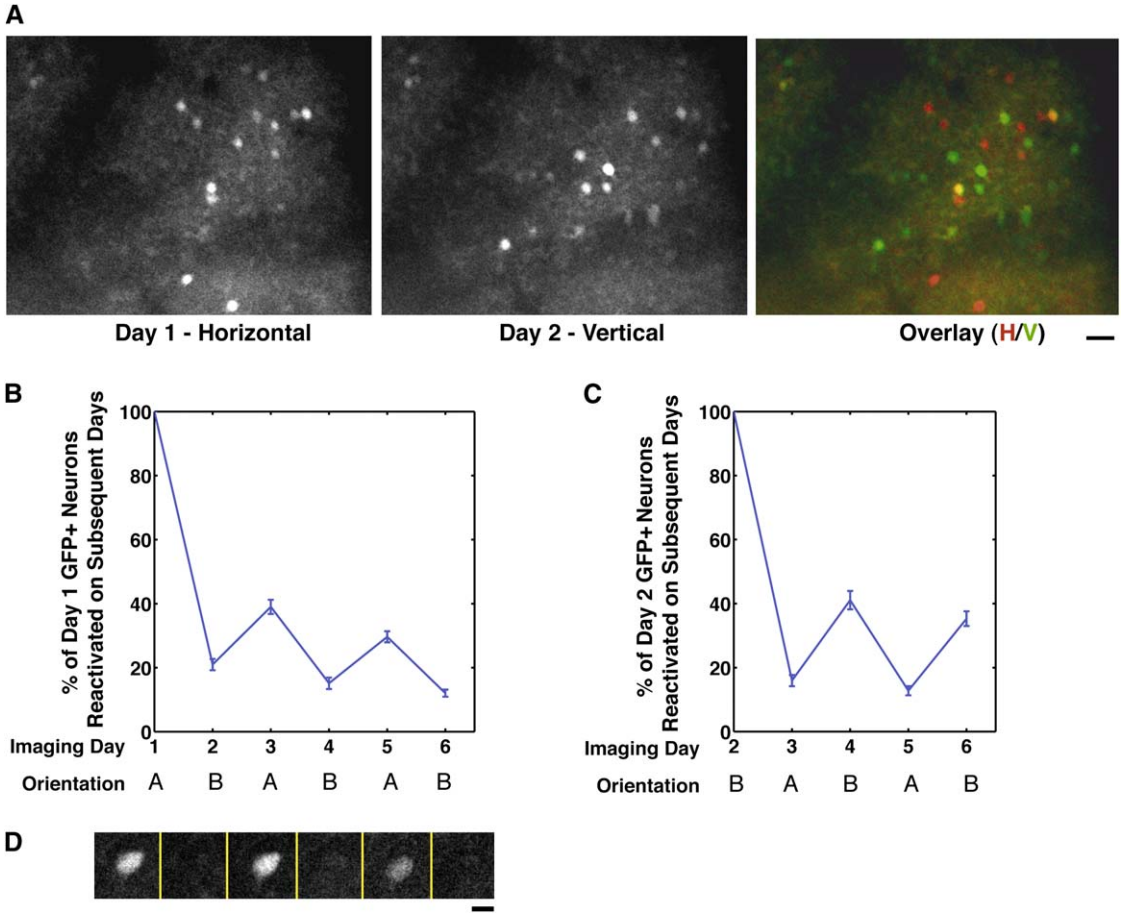

Figure 4. Orientation Specificity of Arc-GFP Response

(A) The alignment of two-photon images taken from the superficial primary visual cortical layers in heterozygous Arc-GFP mice stimulated by horizontal and vertical orientations on two consecutive days shows distinctive activation patterns of GFP+ neurons. The scale bar represents 30 μm.

(B and C) Orientation-specific activation of GFP+ neurons, as determined by the percentage of day 1 (B) or day 2 (C) GFP+ neurons that are reactivated on successive days. Each data point is averaged from 12 regions in six mice.

(D) An example of a neuron that is only activated by horizontal orientation presented on alternate days. The scale bar represents 10 μm.

Error bars indicate SEM.

(Figure 6A, $p < 0.05$, t test with corrections for multiple comparisons, n = 12). When the ratios of the numbers of GFP+ cells in the homozygous versus the heterozygous mice were plotted against the response groups that were arranged approximately in the order of increasing orientation selectivity (Figure 6B), the cells that responded more promiscuously (3:3 and 2:2 groups) gave a mean ratio of 3.5 or higher, while the cells that displayed high orientation selectivity (1:0, 2:0, and 3:0 groups) showed mean ratios close to one. The groups of cells that displayed intermediate levels of selectivity gave mean ratios between 2 and 3.

(D) The reduction of neurons activated on each day depends on the repetition of the same visual experience. Mice were exposed to the same orientation for 3 days, then to an orthogonal orientation on the fourth day. The number of GFP+ neurons activated on each day in each imaged region was compared to that on day 1 as a ratio (n = 8 regions from four mice).

(E) A probability tree constructed from the activation history of neurons that have expressed GFP at least once during the 6 consecutive imaging days in response to the same orientations. The first node represents the population of neurons that express GFP (labeled with "1") on day 1. The color-coded lines connecting this node to its higher daughter nodes represent the proportion of neurons that are either reactivated (leftwards, "1") or inactivated (rightwards, "0"). Each daughter node is further split based on its activation pattern on the next day. The neurons in each node are pooled from 12 regions in six mice.

(F) Neurons that are consistently activated before are more likely to be reactivated.

(G) Neurons that are consistently inactive before are more likely to remain silent.

(H) An example of a neuron that is activated on each of the six days. The scale bar represents 10 μm.

Error bars indicate SEM.

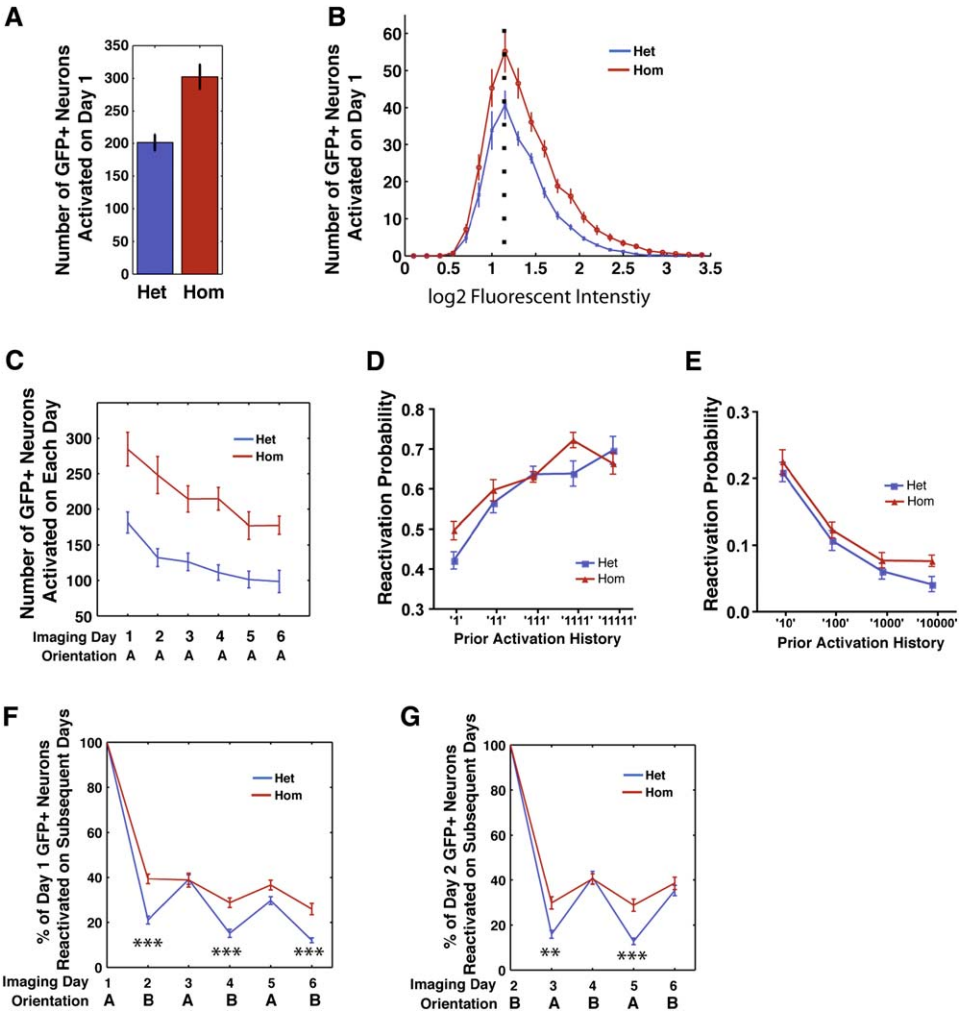

Figure 5. Reduced Orientation Specificity of the Patterns of GFP+ Neurons in Arc Knockout Mice

(A) More GFP+ neurons are activated by a single orientation on day one in the homozygous than that in the heterozygous mice (n = 24 regions from 12 mice, $p < 0.001$, t test).

(B) The fluorescence intensity (I_cell/I_background, see Experimental Procedures) distribution of GFP+ neurons on day one. The number of neurons observed at each intensity level was averaged from 24 regions. The dotted line indicates the intensity level where the peak of the distribution is located, which is the same between the heterozygous and homozygous mice.

(C) More neurons were activated in the homozygous than the heterozygous mice on each day of the SAME orientation experiments, though a gradual reduction of GFP+ neurons was still observed (n = 12).

(D and E) The dependence of neuronal reactivation probability on prior activation history was not significantly different between the heterozygous and homozygous mice (repeated measures two-way ANOVA, $p > 0.05$, n = 12).

(F and G) Higher percentage of neurons was reactivated by the orthogonal orientations in the homozygous compared to the heterozygous mice in the alternate-orientation experiments (***, $p < 0.001$, **, $p < 0.01$, t test with Bonferroni correction for multiple comparisons, n = 12).

All the error bars indicate SEM.

In order to determine whether these differences in the numbers of GFP+ cells is due to a possible effect of Arc (or its absence) on the level of GFP expression in individual neurons, we examined the intensity distribution of GFP+ neurons in the heterozygous and homozygous mice. For this purpose, we pooled cells that responded to both orientations (3:3, 2:2, 1:1, 3:2, 2:1, and 3:1) into one group (the low-orientation-specificity, or LOS, group), and cells that responded to only one orientation (1:0, 2:0, and 3:0) into another (the high-orientation-specificity, or HOS, group), in order to obtain sufficient cell numbers at each fluorescent intensity level. We observed no significant difference in the distribution of GFP+ cells across the whole range of intensity levels in either the LOS or HOS groups (Figures 6C and 6D). As expected, overall there were more GFP+ cells in the homozygous than heterozygous mice in the LOS group (Figure 6D) while no significant difference in the number of GFP+ cell was observed in the HOS group (Figure 6C). The finding that the distribution of GFP+ cells across the levels of GFP expression is not

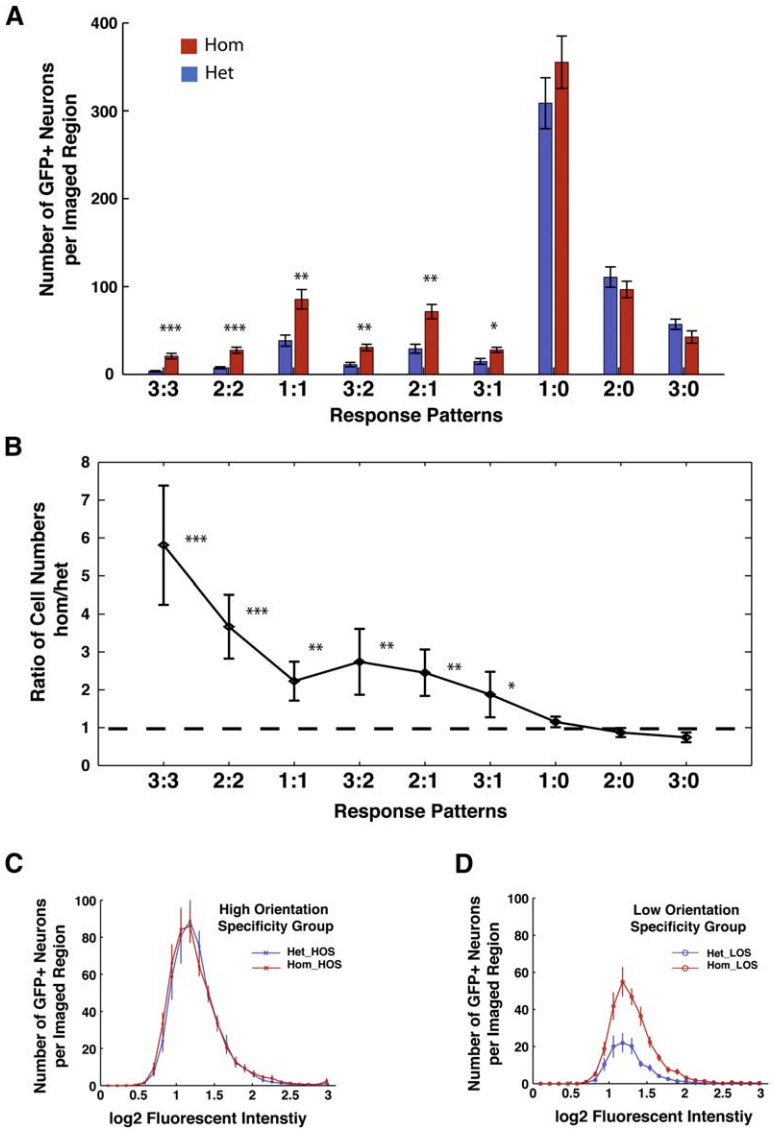

Figure 6. Increased Numbers of GFP+ Neurons with Relatively Low Orientation Specificity in Arc Knockout Mice

(A) GFP+ neurons were classified into nine groups based on their response patterns to horizontal or vertical stripes during the 6-day alternate-orientation experiment. The numbers of cells that responded once, twice, or three times to one specific orientation (1:0, 2:0, 3:0) were not significantly different between the heterozygous and homozygous mice ($p > 0.05$, t test). By contrast, the numbers of cells that responded to both orientations (3:3, 2:2, 1:1, 3:2, 2:1, and 3:1) were significantly higher in the homozygous than the heterozygous mice (t test with Bonferroni correction for multiple comparisons, n = 12 regions; ***, $p < 0.001$; **, $p < 0.01$; *, $p < 0.05$).

(B) The ratios of the numbers of GFP+ cells in the homozygous versus the heterozygous mice were plotted against the response groups that were arranged approximately in the order of increasing orientation selectivity. The ratios were calculated using the average number of cells from 12 regions in each genotype. Error bars indicate standard deviation estimated by bootstrap method.

(C and D) The fluorescence intensity distributions in groups with relatively high orientation specificity ("HOS", pooled from 1:0, 2:0, and 3:0 groups) and relatively low orientation specificity ("LOS", pooled from 3:3, 2:2, 1:1, 3:2, 2:1, and 3:1 groups). The intensity level is the average response of an activated neuron. The number of neurons observed at each intensity level was averaged from 12 regions in six mice. All the error bars indicate SEM.

tilted toward the lower expression side suggests that the increase in the number of GFP+ cells in the LOS group of the homozygous mice is not due to a shift of cells with GFP expression at levels just below the threshold of detection to above the threshold.

Taken together, the lack of Arc in the homozygous mice preferentially increases the number of GFP+ cells with relatively low orientation specificity, and thereby reduces the orientation specificity of the overall neuronal population.

Reduced Orientation Selectivity of Neuronal Spiking Response in Arc Knockout Mice

To determine whether the reduced orientation specificity of Arc-GFP activation patterns in the homozygous mice correlates with a reduction in the orientation selectivity of neuronal spiking responses, we conducted acute extracellular single-unit recordings in the superficial layers of the primary visual cortex of anesthetized wild-type, Arc heterozygous and Arc homozygous mice. In wild-type mice, individual neurons exhibited a wide range of selectivity to oriented gratings (Figures 7A and 7B). In Arc homozygous mice, the distribution of the orientation selectivity index was shifted toward low values (Figure 7B); the median of the index was significantly lower than that in the wild-type and the heterozygous mice ($p < 0.001$, Kruskal-Wallis test). The magnitude of spiking responses at the preferred orientations was not significantly different among the three genotypes ($p > 0.05$, one-way ANOVA) (Figure 7D), nor was the magnitude of spontaneous spiking activities (wt 0.75 ± 0.16, het 0.49 ± 0.07, hom 0.52 ± 0.07, $p > 0.05$, one-way ANOVA). When individual neurons' response tuning curves were normalized and aligned at their preferred orientations, then averaged across the entire population, the resulting average orientation tuning curve was broadened in the Arc homozygous mice (Figure 7C). Together, these electrophysiological data support

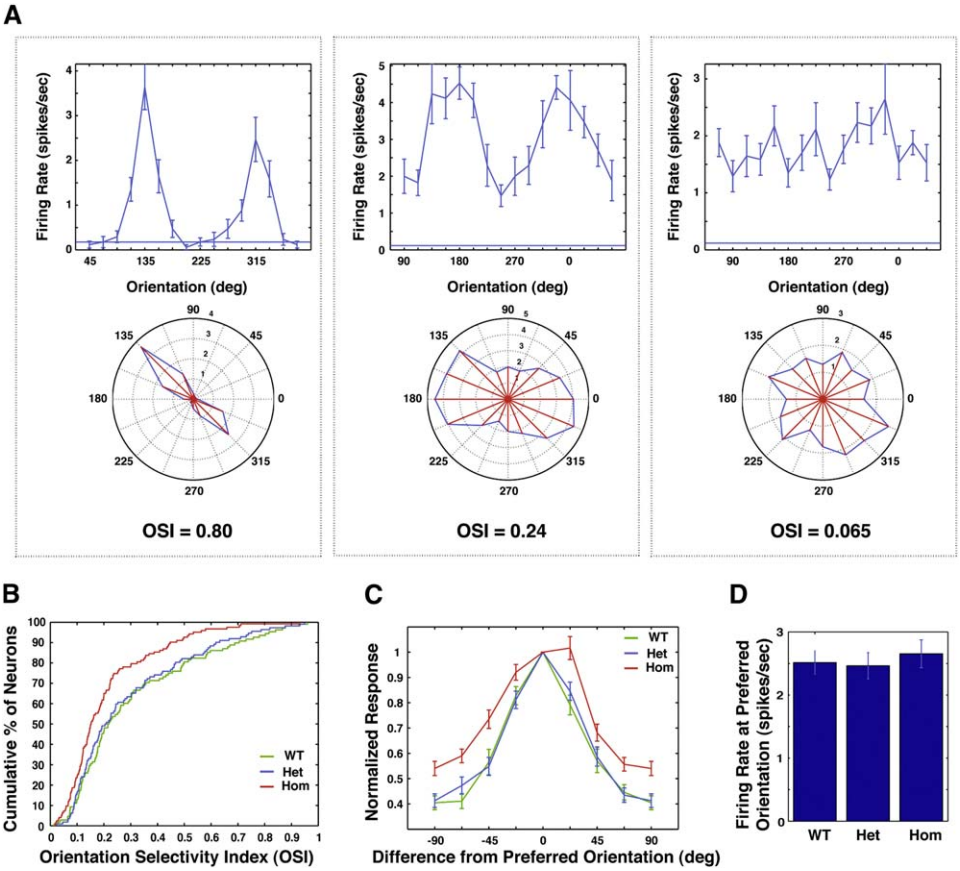

Figure 7. Reduced Orientation Selectivity of Neuronal Spiking Response in Arc Knockout Mice

(A) Examples of cells from wild-type mice that have high, medium, or low orientation selectivity, as determined by single-unit recordings. The background firing rate to a blank screen is indicated by the horizontal line in the linear plot.

(B) The cumulative distribution of the orientation selectivity index is shifted toward lower values in the homozygous compared to the wild-type and heterozygous mice ($p < 0.001$, Kruskal-wallis test for group difference. WT, 6 mice, 108 cells; Het, 6 mice, 112 cells; Hom, 7 mice 123 cells. WT versus Het, $p < 0.001$; Het versus Hom, $p < 0.01$; WT versus Het, $p > 0.05$, Wilcoxon ranksum test with Bonferroni correction for multiple comparisons).

(C) Average spike tuning curves from the wild-type, heterozygous and homozygous mice. Individual neurons' tuning curves were normalized and aligned to their preferred orientation before averaging.

(D) The magnitude of firing rate responses at preferred orientations were not significantly different among the three genotypes ($p > 0.05$, one-way ANOVA). All the error bars indicate SEM.

the conclusion that on average, neurons in Arc homozygous mice are less selective for stimulus orientation.

DISCUSSION

An Arc-Dependent Mechanism for an Enhancement of Orientation Specificity

In this study we have examined the orientation selectivity of visual cortical neurons in wild-type, Arc-GFP heterozygous and Arc-GFP homozygous mice using extracellular single–unit recordings. We found that the percentage of neurons with relatively low orientation selectivity was increased in the homozygous mice (Figure 7B). While neurons in the homozygous mice have normal average firing response to their preferred orientation (Figure 7D), the average orientation-tuning curve is broadened (Figure 7C). Therefore, the presence of Arc protein in normal (i.e., wild-type and heterozygous) mice seems to enhance the overall orientation selectivity of visual cortical neurons.

It is conceivable that the broadening of average orientation tuning curve in the homozygous mice could be due to an increased presence of neurons with low orientation selectivity, a decreased presence of neurons with high orientation selectivity, or a conversion of neurons with high orientation selectivity to those with low orientation selectivity. Through in vivo imaging of the activation patterns of Arc-GFP positive neurons, we were able to differentiate these possibilities. First, we showed that a single orientation activated a larger population of GFP+ neurons (Figures 5A and 5B), and the percentage of GFP+ neurons reactivated by orthogonal orientations increased in the homozygous compared to the heterozygous mice (Figures 5F and 5G), consistent with the differences in average orientation tuning curves (Figure 7C). Second, we found

that the numbers of Arc-GFP-expressing neurons with relatively high orientation specificity were similar between heterozygous and homozygous mice (Figures 6A–6C), while the numbers of neurons with relatively low orientation specificity were significantly greater in the homozygous mice (Figures 6A, 6B, and 6D). This difference in the numbers of GFP+ cells is not due to an influence of Arc on the level of GFP expression in individual neurons, as suggested by the nearly identical distribution of GFP intensity among the cells derived from the mice of the two genotypes (Figures 6C and 6D). Instead, the lack of Arc leads to more GFP+ cells in the population with relatively low orientation specificity across the levels of GFP expression (Figure 6D). These findings suggest that in normal animals, Arc may act as a "molecular filter" to suppress the activation of a significant number of neurons with relatively low orientation specificity, thereby enhancing the overall orientation selectivity of visual cortical neurons.

Together, the single unit recording analysis and the in vivo imaging data provide strong evidence to support a novel physiological function of Arc in enhancing the overall orientation specificity in visual cortex. Since Arc is not expressed in primary visual cortex before eye opening (around postnatal day 14 in mice), nor is it expressed in the thalamus at any age (Lyford et al., 1995; Tagawa et al., 2005), it is very unlikely that Arc is involved in the initial establishment of orientation selectivity that occurs in an experience-independent manner prior to eye opening. The visual experience-dependent increase in orientation selectivity occurs after eye opening (Chapman et al., 1999). In parallel, Arc expression in visual cortex is rapidly induced, which has been shown to be dependent on visual experience (Lyford et al., 1995; Tagawa et al., 2005). Our findings of reduced orientation selectivity in adult (2-4 months of age) Arc homozygous mice compared to the age matched heterozygous mice (Figures 5–7) suggest that Arc plays an important role during this post-eye opening life of an animal.

It is interesting to note that orientation selectivity is also reduced in NR2A and PSD-95 knockout mice (Fagiolini et al., 2003). As the lack of NR2A, PSD-95 and Arc all reduce orientation selectivity in visual cortex and Arc promoter activation is dependent on NMDA-receptor-mediated synaptic inputs (Link et al., 1995; Lyford et al., 1995; Steward and Worley, 2001b), it is possible that NR2A and PSD-95 may be part of the signaling cascade leading to Arc activation.

How Arc acts directly or indirectly to suppress the activation of neurons with low orientation specificity in normal mice is a matter of speculation at this point. One possibility is that Arc reduces the strength of synapses (Rial Verde et al., 2003, Soc. Neurosci., abstract; Shepherd et al., 2004, Soc. Neurosci., abstract) receiving visual inputs. Another is that Arc raises the threshold of cell activation. It is conceivable that either of these potential functions of Arc would have a more pronounced effect on cells with low orientation specificity with respect to suppression of activation, as these cells would, on average, have weaker inputs from any of a number of orientations that they respond to compared to the inputs that cells with high orientation specificity would receive from the specific orientation that they preferentially respond to. Future in vivo studies at the subcellular level and temporally conditional knockout of Arc will be needed to further elucidate its function.

An Arc-Independent Mechanism for Experience-Dependent Adult Cortical Adaptation at the Cellular Ensemble Level

We have observed that in alert adult animals neuronal ensembles expressing Arc-GFP become progressively smaller but more reliable for reactivation with repetition of the same visual experience (Figures 3C–3G). This finding implicates a mechanism for experience-dependent adult visual cortical adaptation at the cellular ensemble level, and provides direct experimental evidence to support the idea that familiar information is compressed in visual cortex after repeated experience (Tsodyks and Gilbert, 2004). Interestingly, although a larger cellular ensemble with reduced orientation specificity was activated in the Arc homozygous mice (Figures 5A–5C and 5F–5G), the number of activated neurons still decreased and the reliability of reactivation improved over repeated exposures to the same stimuli (Figures 5C–5E). These findings suggest that mechanisms independent of Arc control these aspects of experience-dependent activation of neuronal ensembles. For example, it would be interesting to investigate in the future whether the level of global neuromodulators, such as acetylcholine and monoamines (Bao et al., 2001; Weinberger, 2003), could affect the number of reactivated neurons after repeated sensory exposure. In addition, it remains to be studied whether competitive circuit-level mechanisms and/or adaptation in intracellular signaling pathways would contribute to the improvement of the reliability of Arc-GFP activation patterns.

Advantage of the Arc-GFP Imaging System in Studying Experience-Dependent Changes in Cortical Sensory Representations

Experience-dependent changes in cortical sensory representations have been traditionally studied with electrophysiological methods. However, it is difficult to record from the same neurons over several days due to the drifts of chronically implanted electrodes (Emondi et al., 2004). On the other hand, random sampling of neurons with microelectrodes in separately operated animals introduces undesired variations (Sengpiel et al., 1999). To overcome these difficulties, visual fixation-based strategies have been devised with monkeys to identify and compare "experienced" and "inexperienced" neuronal populations in the same animal. Using this strategy enhanced orientation selectivity of neurons in the primary visual cortex of monkeys has been reported after extensive practice of an orientation identification task (Schoups et al., 2001). However, the electrophysiological recordings in this study were conducted only at the end of a month long training

period, not on a daily basis, and the effects of repeated visual experience on orientation selectivity had to be deduced by comparing the properties of two separately located neuronal populations rather than by directly monitoring the changes in the activities of the same neuronal populations.

Our Arc-GFP imaging system provides an alternative method to overcome some of the limitations of these electrophysiological methods, enabling direct and reliable tracking of the response history of the same neurons upon repeated stimulus presentations over multiple days (Figures 3 and 4), as well as offering a broader view of the spatial distribution of activated neurons (Figure S5 in the Supplemental Data available with this article online). Our methods, however, relies on the expression of Arc promoter-driven GFP as the indicator of cellular activation. It has previously been shown that the expression patterns of Arc mRNA as measured by in situ hybridization analysis and place cell spiking patterns as measured by in vivo multi-electrode recording correlated well for the activation of hippocampal neuronal ensembles upon sequential exposure (within 20 min) to two different environments (Guzowski et al., 1999). Whether a similar relationship applies in other brain regions under other behavioral conditions remains to be demonstrated. Our finding that the reduced orientation specificity of Arc-GFP activation patterns is associated with a reduced orientation selectivity of neuronal spiking activities upon a loss of Arc function (Figures 5F, 5G, 7B, and 7C) provides a correlation between Arc gene expression and neuronal spiking activity in visual cortex.

The expression of several other immediate early genes such as c-*fos* and zif-268 have also been used in the literature as an indicator of activated neurons (e.g., Boehm et al., 2005; Choi et al., 2005; Ferguson et al., 2001; Frankland et al., 2004). Although it remains to be shown how neuronal spiking activity is mechanistically related to the activation of these genes, previously published FosGFP transgenic lines (Barth et al., 2004) could be used in a manner similar to the Arc-GFP knockin lines used in this study to track the dynamics of neuronal ensembles in vivo. The combination of molecular genetics, in vivo optical imaging and electrophysiology as applied in our current study provides a powerful approach to advance our understanding of the cellular basis of experience-dependent changes in sensory representations, and bridges the relationship between genes and cognitions.

EXPERIMENTAL PROCEDURES

Generation of Knockin Mice

A 5.5 kb EcoRI/AflII segment of Arc genomic DNA was cloned from a C57/BL6 mouse BAC library (Genomic Systems). A construct containing d2EGFP (Clontech) followed by a Neo cassette was inserted into the NdeI site right after the ATG start codon in the Arc gene. The targeting plasmids were electroporated into a C57/BL6 ES cell line (gift from Dr. Colin Stewart, National Institutes of Health), and homologous recombination was identified by Southern blot. The first 48 base pairs of Arc ORF before the SacII site were deleted as a result of recombination. The Neo cassette was not removed. ES cell clones were injected into Balb/c blastocysts to derive chimeric mice. Germline transmissions of targeting constructs in C57/BL6 mice were identified by coat color and confirmed with Southern blot and PCR.

Mice were normally housed in groups under 12 hr light-dark cycles. Each plastic cage includes a metal rack for water bottle and food pellets. The floor was covered with saw dust and cotton bedding. The light level in the cages was approximately 250 lux. Both heterozygous and homozygous mice were viable and fertile, without overt behavioral abnormality. (There was an earlier report of embryonic lethality in a homozygous Arc knockout mouse line (Liu et al., 2000), but that line was generated differently from a 129/Sv ES cell line.) The loss of Arc mRNA expression in homozygous mice was verified by RT-PCR analysis of brain total RNA preparations, using primers corresponding to both N- and C- terminal coding regions. The loss of Arc protein in homozygous mice was confirmed with both Western blot of brain homogenates (Santa Cruz Biotechnology, rabbit polyclonal antibody against the N-terminal 300 aa. of Arc) and immunofluorescent staining on fixed brain sections (Santa Cruz Biotechnology, goat polyclonal antibodies against the N- and C-terminals of Arc). The expression levels of Arc protein in brain extracts from wild-type and heterozygous littermates were quantified using LICOR's Infrared Western blot imaging system. Linear response ranges were found by serial dilution, then Arc protein level was normalized against the protein level of house keeping enzyme GAPDH, and compared between littermates. GFP immunofluorescent staining was conducted with an anti-GFP antibody (Abcam) on fixed brain sections.

Surgical Preparation

Arc-GFP mice at the age of 2–3 months were surgically implanted with transparent cranial windows over the primary visual cortex (Majewska and Sur, 2003) (Supplemental Experimental Procedures). After surgery, mice were allowed to recover for at least two weeks before visual stimulation and imaging experiments. The animals' care was in accordance with M.I.T. institutional guidelines.

Visual Stimulation

The visual environment to which Arc-GFP mice were exposed consisted of an acrylic cylinder (30 cm in diameter and 60 cm high) lined with alternate black and white stripes (2 cm in width) on the wall. The light level in the cylinder is approximately 250 lux. Mice were transferred in and out of the cylinder in complete darkness by the experimenter wearing infrared goggles.

Two-Photon Microscopy

Two-photon microscopy was performed using a custom built system (Majewska et al., 2000) (Supplemental Experimental Procedures). Laser power was adjusted to the same level (approximately 75 mW) from day to day. Before imaging, each mouse was anesthetized in the dark with isoflurane (4% for induction and 2% for maintenance). It was then transferred onto the microscope stage, with its head fixed using the implanted metal bar to a metal base that connected directly into the microscope stage. A mixture of isoflurane and oxygen was delivered continuously to the mouse through a nose cone. Body temperature was maintained using a heating pad.

For each mouse, we routinely collected two separate image stacks with dimensions of 300 × 400 × 200 μm (width × length × depth) in different areas of V1. The spacing of vertical planes is 5 μm. A typical pyramidal neuron has a diameter of about 10 μm in horizontal dimension and is slightly elongated in the vertical dimension, so that it is sectioned by two to three optical planes.

Image Analysis

To process tens of thousands of images and to reduce potential experimenter bias, we developed an automatic image analysis algorithm (Supplemental Experimental Procedures). To locate individual GFP-expressing cells on each image frame, we used the Difference-of-Gaussian filter (Marr and Hildreth, 1980) to extract signals of one-cell

diameter (20 pixels or 10 μm) from their surrounding background (Figure S1). Typically, there were 5–20 visually identified GFP+ cells per image (600 × 800 pixels), and the area of each cell was approximately 300 pixels. Therefore, only 1.25% (20 × 300/600/800) or less of an image was occupied by GFP+ cells, and most pixels in the filtered image had intensity values varying around zero. The median of the absolute intensity variations in the filtered image was calculated to derive a robust estimator of the standard deviation (SD) of the background noise (Huber, 1981). The 3D coordinates of local intensity peaks above 4.6 × SD were identified in the filtered images, and only the one with the highest intensity value for each cell position was used to represent the center of an activated cell expressing GFP. Therefore, each GFP-expressing cell was only counted once in the 3-D image stacks.

We set the threshold for cell detection at 4.6 × SD to minimize false-positive rates. Based on Gaussian random field theory that has been widely applied in medical imaging research (Worsley et al., 1992), the average number of false positive peaks at this threshold is below 0.05 per filtered image, less than 1% (0.05/5) of the number of GFP+ cells per image. After setting this threshold, we confirmed that the intensity distribution of randomly sampled GFP- spots was well separated from that of all the GFP+ neurons in the imaged region (Figure S2D). We also compared the automatic cell detection algorithm to human manual counting and found that 94% (1569/1666) of cells detected by a human observer blind to the experimental parameters were captured by the algorithm.

To further examine the robustness of the orientation-specific neuronal reactivation curves in the heterozygous and homozygous Arc-GFP mice (Figures 5F and 5G), we analyzed our whole data set using various threshold values for automatic cell detection. The results showed that the shapes of the reactivation curves were robust across a range of threshold choices (from 4.0 × SD to 7.0 × SD, Figure S8).

To quantify the fluorescent intensity of an identified GFP+ cell, we first defined a cell area that included all the pixels with intensity levels higher than half of the peak intensity value and within 15 pixels from the center (Figure S2A). The mean pixel intensity in the cell area is calculated as I_cell. A background area was defined as a ring between 15 and 20 pixels from the center. If a part of a neighboring cell was located in the background area, that area was excluded from calculation. The mean pixel intensity in the background area is calculated as I_background. The GFP intensity signal of a cell was calculated as I_cell/I_background. The denominator normalized the GFP signal against background variations in laser power or tissue light-scattering properties (Jähne, 2002). We have also quantified I_background and I_cell using alternative size and shape definitions, and obtained similar intensity distributions (Figure S9).

Images belong to the same time series were first aligned at the microscope stage, using idiosyncratic vasculature patterns and stable auto-fluorescent signals (Grutzendler et al., 2002; Trachtenberg et al., 2002). Further refinement was conducted after image acquisition using 3D affine transformation. Cell centroids calculated from different time points were merged if they were within one cell diameter of each other.

In Vivo Electrophysiology

Wild-type, heterozygous, and homozygous Arc-GFP mice (3–4 months old) were prepared for extracellular microelectrode recordings following procedures adapted from published reports (Gordon and Stryker, 1996) (Supplemental Experimental Procedures). Single-unit recordings were conducted with tungsten microelectrodes (2–4 MΩ resistance, FHC) as previously described (Dragoi et al., 2000). For each animal, we recorded approximately 15–20 cells in four or five penetrations in the superficial layers (less than 350 μm from pial surface) of primary visual cortex. High-contrast square wave gratings were presented to anesthetized mice on a computer monitor at orientations 22.5° apart with a spatial frequency of 0.05 cycle/degree and a temporal frequency of 3 Hz. During each trial, all 16 gratings and a blank screen of uniform intermediate gray were randomly interleaved, and presented for 2 s each, with 500 ms intervals between each stimulus. In total 10 trials were presented to each cell. Firing rate responses to each orientation were averaged from those trials, and spontaneous activity was subtracted. The orientation selectivity index (OSI) was calculated using a vector averaging method, and the preferred orientation was determined from the angle of the mean orientation vector (Dragoi et al., 2000).

Supplemental Data

Supplemental Data include Supplemental Experimental Procedures, nine figures, and Supplemental References and can be found with this article online at http://www.cell.com/cgi/content/full/126/2/389/DC1/.

ACKNOWLEDGMENTS

We thank Dr. Arvind Govindarajan and members of Tonegawa and Sur laboratories for discussions and critical readings and editing of the manuscript, and Chanel Lovett for technical assistance. This work was supported by an NIH Silvio O. Conte Center grant (P50-MH58880) to S.T., a Wills Foundation fellowship to K.H.W., grants from the NIH and the Simons Foundation to M.S., and NIH grants AI24643 and AI51164 to C.H. S.T. is an investigator of Howard Hughes Medical Institute and RIKEN-MIT Neuroscience Research Center.

Received: August 31, 2005
Revised: January 16, 2006
Accepted: June 5, 2006
Published: July 27, 2006

REFERENCES

Bao, S., Chan, V.T., and Merzenich, M.M. (2001). Cortical remodelling induced by activity of ventral tegmental dopamine neurons. Nature *412*, 79–83.

Barth, A.L., Gerkin, R.C., and Dean, K.L. (2004). Alteration of neuronal firing properties after in vivo experience in a FosGFP transgenic mouse. J. Neurosci. *24*, 6466–6475.

Boehm, U., Zou, Z., and Buck, L.B. (2005). Feedback loops link odor and pheromone signaling with reproduction. Cell *123*, 683–695.

Chapman, B., Godecke, I., and Bonhoeffer, T. (1999). Development of orientation preference in the mammalian visual cortex. J. Neurobiol. *41*, 18–24.

Choi, G.B., Dong, H.W., Murphy, A.J., Valenzuela, D.M., Yancopoulos, G.D., Swanson, L.W., and Anderson, D.J. (2005). Lhx6 delineates a pathway mediating innate reproductive behaviors from the amygdala to the hypothalamus. Neuron *46*, 647–660.

Crair, M.C., Gillespie, D.C., and Stryker, M.P. (1998). The role of visual experience in the development of columns in cat visual cortex. Science *279*, 566–570.

Dragoi, V., Sharma, J., and Sur, M. (2000). Adaptation-induced plasticity of orientation tuning in adult visual cortex. Neuron *28*, 287–298.

Emondi, A.A., Rebrik, S.P., Kurgansky, A.V., and Miller, K.D. (2004). Tracking neurons recorded from tetrodes across time. J. Neurosci. Methods *135*, 95–105.

Fagiolini, M., Katagiri, H., Miyamoto, H., Mori, H., Grant, S.G., Mishina, M., and Hensch, T.K. (2003). Separable features of visual cortical plasticity revealed by N-methyl-D-aspartate receptor 2A signaling. Proc. Natl. Acad. Sci. USA *100*, 2854–2859.

Ferguson, J.N., Aldag, J.M., Insel, T.R., and Young, L.J. (2001). Oxytocin in the medial amygdala is essential for social recognition in the mouse. J. Neurosci. *21*, 8278–8285.

Frankland, P.W., Bontempi, B., Talton, L.E., Kaczmarek, L., and Silva, A.J. (2004). The involvement of the anterior cingulate cortex in remote contextual fear memory. Science *304*, 881–883.

Gordon, J.A., and Stryker, M.P. (1996). Experience-dependent plasticity of binocular responses in the primary visual cortex of the mouse. J. Neurosci. *16*, 3274–3286.

Grutzendler, J., Kasthuri, N., and Gan, W.B. (2002). Long-term dendritic spine stability in the adult cortex. Nature *420*, 812–816.

Guzowski, J.F., Lyford, G.L., Stevenson, G.D., Houston, F.P., McGaugh, J.L., Worley, P.F., and Barnes, C.A. (2000). Inhibition of activity-dependent arc protein expression in the rat hippocampus impairs the maintenance of long-term potentiation and the consolidation of long-term memory. J. Neurosci. *20*, 3993–4001.

Guzowski, J.F., McNaughton, B.L., Barnes, C.A., and Worley, P.F. (1999). Environment-specific expression of the immediate-early gene Arc in hippocampal neuronal ensembles. Nat. Neurosci. *2*, 1120–1124.

Guzowski, J.F., Miyashita, T., Chawla, M.K., Sanderson, J., Maes, L.I., Houston, F.P., Lipa, P., McNaughton, B.L., Worley, P.F., and Barnes, C.A. (2006). Recent behavioral history modifies coupling between cell activity and Arc gene transcription in hippocampal CA1 neurons. Proc. Natl. Acad. Sci. USA *103*, 1077–1082.

Hubel, D.H., and Wiesel, T.N. (1962). Receptive fields, binocular interaction and functional architecture in the cat's visual cortex. J. Physiol. *160*, 106–154.

Hubel, D.H., and Wiesel, T.N. (1963). Receptive Fields of Cells in Striate Cortex of Very Young, Visually Inexperienced Kittens. J. Neurophysiol. *26*, 994–1002.

Huber, P.J. (1981). Robust Statistics (New York: Wiley).

Jähne, B. (2002). Digital Image Processing, Fifth Edition (Berlin and New York: Springer).

Li, X., Zhao, X., Fang, Y., Jiang, X., Duong, T., Fan, C., Huang, C.C., and Kain, S.R. (1998). Generation of destabilized green fluorescent protein as a transcription reporter. J. Biol. Chem. *273*, 34970–34975.

Link, W., Konietzko, U., Kauselmann, G., Krug, M., Schwanke, B., Frey, U., and Kuhl, D. (1995). Somatodendritic expression of an immediate early gene is regulated by synaptic activity. Proc. Natl. Acad. Sci. USA *92*, 5734–5738.

Liu, D., Bei, D., Parmar, H., and Matus, A. (2000). Activity-regulated, cytoskeleton-associated protein (Arc) is essential for visceral endoderm organization during early embryogenesis. Mech. Dev. *92*, 207–215.

Lyford, G.L., Yamagata, K., Kaufmann, W.E., Barnes, C.A., Sanders, L.K., Copeland, N.G., Gilbert, D.J., Jenkins, N.A., Lanahan, A.A., and Worley, P.F. (1995). Arc, a growth factor and activity-regulated gene, encodes a novel cytoskeleton-associated protein that is enriched in neuronal dendrites. Neuron *14*, 433–445.

Majewska, A., and Sur, M. (2003). Motility of dendritic spines in visual cortex in vivo: changes during the critical period and effects of visual deprivation. Proc. Natl. Acad. Sci. USA *100*, 16024–16029.

Majewska, A., Yiu, G., and Yuste, R. (2000). A custom-made two-photon microscope and deconvolution system. Pflugers Arch. *441*, 398–408.

Marr, D., and Hildreth, E. (1980). Theory of edge detection. Proc. R. Soc. Lond. B. Biol. Sci. *207*, 187–217.

Moga, D.E., Calhoun, M.E., Chowdhury, A., Worley, P., Morrison, J.H., and Shapiro, M.L. (2004). Activity-regulated cytoskeletal-associated protein is localized to recently activated excitatory synapses. Neuroscience *125*, 7–11.

Schoups, A., Vogels, R., Qian, N., and Orban, G. (2001). Practising orientation identification improves orientation coding in V1 neurons. Nature *412*, 549–553.

Sengpiel, F., Stawinski, P., and Bonhoeffer, T. (1999). Influence of experience on orientation maps in cat visual cortex. Nat. Neurosci. *2*, 727–732.

Steward, O., and Worley, P.F. (2001a). A cellular mechanism for targeting newly synthesized mRNAs to synaptic sites on dendrites. Proc. Natl. Acad. Sci. USA *98*, 7062–7068.

Steward, O., and Worley, P.F. (2001b). Selective targeting of newly synthesized Arc mRNA to active synapses requires NMDA receptor activation. Neuron *30*, 227–240.

Sutton, M.A., Wall, N.R., Aakalu, G.N., and Schuman, E.M. (2004). Regulation of dendritic protein synthesis by miniature synaptic events. Science *304*, 1979–1983.

Tagawa, Y., Kanold, P.O., Majdan, M., and Shatz, C.J. (2005). Multiple periods of functional ocular dominance plasticity in mouse visual cortex. Nat. Neurosci. *8*, 380–388.

Trachtenberg, J.T., Chen, B.E., Knott, G.W., Feng, G., Sanes, J.R., Welker, E., and Svoboda, K. (2002). Long-term in vivo imaging of experience-dependent synaptic plasticity in adult cortex. Nature *420*, 788–794.

Tsodyks, M., and Gilbert, C. (2004). Neural networks and perceptual learning. Nature *431*, 775–781.

Wallace, C.S., Lyford, G.L., Worley, P.F., and Steward, O. (1998). Differential intracellular sorting of immediate early gene mRNAs depends on signals in the mRNA sequence. J. Neurosci. *18*, 26–35.

Weinberger, N.M. (2003). The nucleus basalis and memory codes: auditory cortical plasticity and the induction of specific, associative behavioral memory. Neurobiol. Learn. Mem. *80*, 268–284.

White, L.E., Coppola, D.M., and Fitzpatrick, D. (2001). The contribution of sensory experience to the maturation of orientation selectivity in ferret visual cortex. Nature *411*, 1049–1052.

Worsley, K.J., Evans, A.C., Marrett, S., and Neelin, P. (1992). A three-dimensional statistical analysis for CBF activation studies in human brain. J. Cereb. Blood Flow Metab. *12*, 900–918.